Published in final edited form as:
Sci Signal. ; 4(163): ra13. doi:10.1126/scisignal.2001518.

Ubiquitination of Ras enhances activation and facilitates binding to select downstream effectors

Atsuo T. Sasaki[1,3], **Arkaitz Carracedo**[2,6], **Jason W. Locasale**[1,3], **Dimitrios Anastasiou**[1,3], **Koh Takeuchi**[4,7], **Emily Rose Kahoud**[1], **Sasson Haviv**[1], **John M. Asara**[1,5], **Pier Paolo Pandolfi**[2], and **Lewis C. Cantley**[1,3,*]

[1]Division of Signal Transduction, Beth Israel Deaconess Medical Center, Harvard Medical School, Boston, Massachusetts 02115

[2]Departments of Medicine and Pathology, Beth Israel Deaconess Medical Center, Harvard Medical School, Boston, Massachusetts 02115

[3]Department of Systems Biology, Harvard Medical School, Boston, Massachusetts 02115

[4]Department of Biological Chemistry and Molecular Pharmacology, Harvard Medical School, Boston, Massachusetts 02115

[5]Department of Medicine, Harvard Medical School, Boston, Massachusetts 02115

Abstract

GTP-loaded Ras induces multiple signaling pathways by binding to its numerous effectors such as Raf and PI3K. Ras activity can be influenced by activation of Ras-GEFs that stimulate GDP release and GTP loading or by inhibition of Ras-GAPs that stimulate GTP hydrolysis. Here, we report that monoubiquitination of Lys^{147} within the G domain of wild-type K-Ras, the Ras gene most frequently mutated in cancer, leads to enhanced GTP loading. Furthermore, ubiquitination increases the ability of the oncogenic Gly-12-Val mutant of K-Ras to bind the downstream effectors PI3K and Raf. These results indicate that monoubiquitination both enhances GTP loading on K-Ras and increases its affinity for specific downstream effectors, providing a previously unidentified mechanism for Ras activation.

Keywords

G-protein; Ubiquitin; Ras; PI3K; Raf

INTRODUCTION

The most frequently mutated oncogenes in the deadliest cancers responsible for human mortality are *KRAS, PIK3CA* and *BRAF*. Importantly the signaling enzymes encoded by *PIK3CA* and *BRAF* are, in part, regulated by direct binding to activated forms of the Ras

*Correspondence to be addressed to: Division of Signal Transduction, Beth Israel Deaconess Medical Center, Department of Systems Biology, Harvard Medical School, Boston, Massachusetts 02115, Tel: 617-735-2601, fax: 617-735-2646, lcantley@hms.harvard.edu.
[6]Current addresses: CIC bioGUNE, Technology Park of Bizkaia, 48160 Derio, Bizkaia, Spain.
[7]Biomedicinal Information Research Center, National Institute of Advanced Industrial Science and Technology, 2-3-26 Aomi, Koto, Tokyo 135-0064, Japan.

Competing interests: The authors declare that they have no competing interests.

Author contributions: A.T.S. designed, performed experiments and analyzed data; A.C. performed xenograft assay; J.W.L. performed bioinformatics; E.R.K., S.H. assisted experiments; D.A., K.T., P.P.P., L.C.C. helped to raise a model; L.C.C. wrote the paper.

proteins suggesting that dysregulation of this key step in signaling is critical for tumor formation. Ras acts as a molecular switch that is activated upon GTP loading and deactivated upon hydrolysis of GTP to GDP. This switch mechanism is common to a wide variety of GTP-binding proteins and is mediated by a conserved structure called the G-domain that consists of five conserved G boxes. Under physiological conditions, the rate of GDP or GTP release from the G-domain is slow. As a consequence the GDP produced by GTP hydrolysis on Ras is trapped and the bulk of cellular Ras accumulates in the GDP-bound 'off' state, despite the high GTP/GDP ratio in the cytosol (1–3). Growth factors can turn on Ras by activating Guanine nucleotide Exchange Factors (GEFs) or by inhibiting the GTPase Activating Proteins (GAPs) or by both mechanisms. RasGEFs bind to Ras and lower the transition energy for the nucleotide exchange of the bound GDP for the more abundant cytosolic GTP, whereas RasGAPs bind to Ras and catalyze GTP hydrolysis. The most prevalent oncogenic mutations in Ras (Gly^{12} and Gly^{13} in the G1 box, and Gln^{61} in the G3 box) preserve the GTP bound state by inhibiting intrinsic GTPase activity and by interfering with the ability of GAPs. Other less frequently observed mutations, such as those found in the G4 and G5 boxes, increase the rate of nucleotide exchange, thereby mimicking the GEFs and increasing the GTP-bound state (1–7).

Activated Ras controls diverse signaling pathways that ultimately determine Ras-induced cellular responses such as cell proliferation, survival, differentiation and motility. These multiple Ras functions depend on its binding to a range of functionally diverse effector molecules such as Raf, PI3K, AF6 and RASSFs (1). The enhancement of specific effector pathways plays a critical role in maintaining an appropriate biological response (8). The specificity in Ras-induced signaling is primarily determined by the balance between Ras affinity for each of its effectors and the local concentrations of those effectors. In addition, scaffold proteins have been shown to guide activation of specific effector pathway(s). For example, SHOC2/Sur-8 bridges Ras and Raf to specifically enhance the Raf/MEK/ERK pathway without enhancing PI3K/AKT signaling (9, 10).

Recently, ubiquitination of Ras has been shown to control Ras protein levels and subcellular localization. The endosomal E3-ligase, Rabex5/RabGEF1 promotes mono- and di-ubiquitination of H-Ras and N-Ras, leading to endosomal Ras anchoring (11, 12). The F-box protein β−TrCP mediates poly-ubiquitination of all Ras isoforms, leading to a proteasome-dependent degradation of Ras (13). Ubiquitination, like phosphorylation, is a dynamic modification and could potentially change the conformation and activity of the target proteins. However, these previous studies did not address the predominant sites of ubiquitination or the possibility that ubiquitination at specific sites could affect the activation state of Ras.

To better understand Ras signaling, we examined the possibility that ubiquitination of Ras could affect its nucleotide-binding state and its interactions with downstream effectors. Here, we used a mass-spectrometry based approach to identify Ras ubiquitination sites and examined the function of site-specific ubiquitination on Ras. We discovered two surprising consequences of monoubiquitination: an increase in the fraction of GTP-bound Ras and selective enhancement of Ras binding to specific effectors.

RESULTS

Tandem mass spectrometry analysis of K-Ras and H-Ras identified Lys^{147} as one of the major ubiquitination sites

To examine whether endogenous K-Ras and H-Ras are ubiquitinated, His-tagged ubiquitin was expressed in HEK293T cells and purified by metal ion affinity chromatography. The expression level of His-ubiquitin was comparable to that of endogenous ubiquitin (Fig.1A

left). We found that endogenous K-Ras and H-Ras underwent mono-ubiquitination in HEK293T cells. Di-ubiquitinated Ras was also detected but the amount was less than the mono-ubiquitinated form (Fig.1A right). To investigate whether Ras ubiquitination is modulated by Ras downstream signaling, the T35A-K-Ras mutant that impairs GTP-mediated switch transition and effector binding (fig. S1A) (14) was expressed in HEK293T cells. T35A-K-Ras underwent ubiquitination at a similar level to WT-K-Ras (fig. S1B), suggesting that K-Ras ubiquitination occurs independently of its activity.

We utilized an unbiased mass spectrometry-based approach to identify ubiquitination sites of Ras. His-tagged ubiquitin and Flag-tagged K-Ras4B (K-Ras hereafter) were expressed in HEK293T cells at levels similar to endogenous K-Ras (Fig. 1B) and subjected to sequential affinity chromatography. His-ubiquitinated proteins were purified by Co^{2+} metal affinity chromatography in 8M urea denaturing conditions. His-ubiquitinated K-Ras was subsequently purified with anti-Flag resin. Following purification, mono- and di-ubiquitinated K-Ras appeared to be the major ubiquitination forms, which is consistent with the endogenous K-Ras ubiquitination pattern (Fig. 1, A and B). H-Ras ubiquitination sites were also determined by the same approach. Tandem mass spectrometric analysis of tryptic fragments from the bands migrating at the positions expected for mono- and di-ubiquitinated Ras revealed ubiquitination at Lys residues 104 and 147 of K-Ras, and Lys residues 117, 147 and 170 for H-Ras (fig. S1C). The tryptic peptide with ubiquitination at Lys^{147} (K147) was the most frequently observed peptide for both K-Ras and H-Ras, while Lys^{117} appeared as a secondary major ubiquitination site in H-Ras.

Mass spectrometry analysis detected Lys^{48}-linked ubiquitin-linkage in the di-ubiquitinated forms of both K-Ras and H-Ras indicating that at least some of the di-ubiquitinated Ras is due to tandem modification. However, we could not rule out the possibility that some of the di-ubiquitinated Ras consisted of two separate mono-ubiquitinations at different lysine residues on Ras, and that there could be other ubiquitin linkage, such as Lys^{63}-linked ubiquitin, which was not detected by current mass spectrometry sensitivity. It is worth noting that Lys^{48}-linked proteasome-dependent degradation needs at least four ubiquitin moieties to be recognized by the proteasome (15, 16).

Ubiquitination of Lys^{147}, a conserved lysine in the G5 box, increases the fraction of GTP-bound Ras

Interestingly, two major ubiquitination sites, Lys^{117} and Lys^{147}, are conserved in the G4 and G5 boxes, respectively and are critical for the tight binding of Ras to GDP or GTP (2–7) (Fig. 1, C and D). Oncogenic mutations at these sites, namely K117R and K117N, have been found in human cancers. These mutations reduce the binding affinity for GTP and GDP which, in turn increases the GTP-bound form as the cellular concentration of GTP is generally much higher than that of GDP (5, 6, 17). Other activating mutations in the Ras-G5 domain, A146T and A146V, which are proximal to the identified ubiquitination site, Lys^{147}, have also been found in human cancers. Similar to the K117R/N mutation, Ala^{146} Ras mutants result in an increase of the GTP-form (4, 7, 17–20). Importantly, as a part of the "SAK" motif in the G5-box, the long aliphatic side chain of Lys^{147} stabilizes the binding of Ras to the guanine moiety of the nucleotide (21, 22). This suggests that Lys^{147} itself is critical for stabilizing GDP binding to inactive Ras and that either a modification of Lys^{147} or amino acid substitution at this position could allow spontaneous GDP/GTP exchange in the absence of a GEF.

To examine this possibility, we employed a pull-down assay using the Ras binding domain (RBD) from amino acids 1–149 of human Raf1 kinase fused to GST, which preferentially binds to GTP-loaded Ras (23). Strikingly, mutation of Lys^{147} to alanine or arginine resulted in increased Ras binding to the RBD (Fig. 1E). The activation levels of K147A and K147R

were different, suggesting that the increased activation is not due to lack of ubiquitination at Lys^{147}, but is due to the relative effects of these two substitutions on the conformation of the G5 box. These results are consistent with the model stated above and raise the possibility that a post-translational modification of Lys-147, could either further stabilize GDP binding and prevent Ras activation, or could have a similar effect to the amino acid substitutions and allow spontaneous GDP release in the absence of a GEF.

To examine the effect of ubiquitination on GTP loading, we purified wild-type K-Ras, oncogenic G12V-K-Ras mutant or the ubiquitinated subfraction of wild-type K-Ras from ^{32}P-orthophosphate labeled cells and utilized thin layer chromatography (TLC) and high performance liquid chromatography (HPLC) to assess the ratio of ^{32}P-GTP to ^{32}P-GDP that co-purified with each form of K-Ras. As expected based on previous studies, wild-type K-Ras bound primarily ^{32}P-GDP, while G12V-Ras bound ^{32}P-GTP (Fig.2, A and B). Interestingly, the ubiquitinated subfraction of wild-type K-Ras retained a significant amount of ^{32}P-GTP. These results are consistent with a model in which ubiquitination of Lys^{147} (or Lys^{117}), destabilizes GDP binding, allowing spontaneous GDP/GTP exchange. It could be argued that GTP loading occurs prior to ubiquitination and that the GTP bound form of K-Ras, via interaction with effectors, is preferentially mono-ubiquitinated via a feedback mechanism. While it is difficult to eliminate this possibility, it is unlikely since, as shown in fig. S1B, the T35 mutant of K-Ras, which fails to interact with downstream effectors (fig. S1B) undergoes comparable monobuiquitination to wild type Ras. These results, along with the crystal structure, support a model in which mono-ubiquitination at a Lys residue directly involved in GDP binding either enhances nucleotide exchange on K-Ras, impairs GTP hydrolysis, or both.

To corroborate this finding, we measure the activity of Ras by the GST-RBD pull-down assay. To ensure that ubiquitinated Ras was being detected, the protein pulled down by GST-RBD was subjected to a second affinity purification on a cobalt column to purify the Flag-His-tagged K-Ras. As predicted, only a very small fraction of wild-type K-Ras was pulled down by the GST-RBD (Fig. 2C and fig. S1D), consistent with very little wild-type K-Ras being in the GTP state under these conditions (Fig.2, A and B). However, a much greater fraction of the ubiquitinated-K-Ras was pulled down by the GST-RBD (Fig. 2C and fig. S1D). These results are consistent with a greater fraction of ubiquitinated K-Ras being in the GTP state (Fig. 2, A and B).

Some G-proteins, such as Rac1, have leucine at the position equivalent to Lys^{147} in Ras. As occurs with Lys^{147}, the long aliphatic side chain of Leu^{160} of Rac1 interacts with the guanine moiety of the nucleotide (2, 3) (Fig. 1, C and D). This suggests that a K147L mutant of K-Ras may retain similar basal activity for wild-type K-Ras. We have observed that non-ubiquitinated K147L-K-Ras actually has similar basal affinity to the RBD compared to non-ubiquitinated WT-K-Ras (Fig. 2C), and that the kinetics of EGF-mediated activation of K147L and WT-K-Ras are similar (fig. S2A). This suggests that the GDP/GTP cycle of K147L-K-Ras is not affected. The K147L mutant of K-Ras still undergoes mono-ubiquitination (presumably due to modification at Lys^{117} and other sites); however, mono-ubiquitinated K147L-K-Ras shows a reduced ability to bind to the RBD relative to the mono-ubiquitinated WT-K-Ras. This result indicates that ubiquitination at Lys^{147} plays a dominant role in promoting binding to the RBD but does not eliminate the possibility that modification at other sites could also contribute.

Importantly, in addition to K-Ras4B, mono- and di- ubiquitinated forms of the other three Ras isoforms (K-Ras4A, H-Ras and N-Ras) had increased GTP-forms (Fig. 2D and fig, S1D). We have also shown that ubiquitinated H-Ras, like ubiquitinated K-Ras, has increased ^{32}P-GTP/GDP ratio compared to non-ubiquitinated H-Ras (fig, S1E). The

activation levels of ubiquitinated Ras isoforms were variable, suggesting that each Ras isoform may have a distinctive ubiquitination site, or undergoes isoform-specific regulation, presumably due to differential subcellular localization and/or binding proteins.

Ubiquitinated Ras activates Raf and PI3K more efficiently than non-ubiquitinated Ras

Although the results above indicate that the bulky 8.5 kDa ubiquitin moiety bound to Lys^{147} of K-Ras did not interfere with *in vitro* binding to the RBD domain, they do not address whether ubiquitinated K-Ras is capable of binding and activating endogenous effectors such as c-Raf or PI3K *in vivo*. To address the effect of K-Ras ubiquitination on its binding to PI3K and Raf family members, either total G12V-K-Ras or the ubiquitinated subfraction of G12V-K-Ras was immunoprecipitated and the immunoprecipitates were probed with antibodies to detect associated Ras effector molecules. Since the majority of G12V-K-Ras is already in the GTP state (Fig. 2, A and B), any difference observed is likely due to ubiquitination. Surprisingly, endogenous Raf kinases, RalGDS, and the p85 subunit of PI3K were readily detected in the immunoprecipitate of ubiquitinated G12V-K-Ras, despite there being far less mono-ubiquitinated G12V-K-Ras compared to total G12V-K-Ras in the two precipitates (Fig. 3 and fig, S2). K-Ras has been shown to interact with PLCε, Afadin, Calmodulin and Tubulin (1, 24–26). We observed that endogenous PLCε, Afadin, Calmodulin and Tubulin co-immunoprecipitated with G12V-K-Ras, however, these proteins were not enriched in the immunoprecipitate of ubiquitinated G12V-K-Ras. This indicates that ubiquitinated G12V-K-Ras does not have a specific affinity toward these proteins, and that ubiquitination of K-Ras results in preferential association with PI3K, Raf and RalGDS family members.

To examine whether the binding of ubiquitinated K-Ras to Raf and PI3K inhibits or can actually enhance their kinase activity, both total G12V-K-Ras and the ubiquitinated subfraction of G12V-K-Ras were purified from cell lysates and subjected to an *in vitro* kinase (I.V.K.) assay (Fig. 4A). Even though far less ubiquitinated-K-Ras than total K-Ras was immunoprecipitated, the ubiquitinated K-Ras immunoprecipitate contained comparable PI3K and Raf kinase activities. Sequential dilutions of the total K-Ras fraction to levels similar to that in the ubiquitinated K-Ras precipitate resulted in almost undetectable PI3K and Raf kinase activities. Taken together, these results suggest that ubiquitinated GTP-K-Ras binds more tightly to activate these effectors than non-ubiquitinated GTP-K-Ras does, or that the ubiquitin moiety plays an additional role in stimulating the activity of the bound effectors.

How does ubiquitination enhance Ras binding to specific effectors? The GST-RBD protein did not preferentially pull down ubiquitinated G12V-K-Ras compared to non-ubiquitinated G12V-K-Ras (fig, S1F), indicating that the minimal RBD of Raf does not confer specificity for the ubiquitinated form of Ras. We next asked if regions of Raf1 C-terminal of the RBD conferred preferential affinity for ubiquitinated Ras by expressing constructs that included 1–149 (the same region used for the GST-RBD construct), 1–256 and 1–330 of Raf1 as GFP fusions. Ubiquitinated G12V-K-Ras and total G12V-K-Ras were purified from cells expressing the GFP-Raf1 fusion proteins. The total G12V-K-Ras bound to all three Raf constructs (Fig. 4B), though the Raf1–256 construct was preferentially bound compared to its level of expression, in agreement with previous studies (27–29). Remarkably, the ubiquitinated K-Ras bound to the 1–256, 1–330 constructs much more strongly than to the 1–149 construct (Fig. 4B). These results suggest that the extended region of the RBD substantially increases the affinity for ubiquitinated Ras, possibly through a second contact with a region of Raf C-terminal of the RBD to enhance the association between activated Ras and Raf.

Ubiquitination of K-Ras may change its subcellular localization and elicit signaling at specific subcellular locations as reported recently (11, 12). To test this possibility, GFP-tagged G12V/K147L-K-Ras and RFP-tagged G12V-K-Ras were co-expressed and their intracellular locations were compared by confocal microscopy (fig, S3A). In general, the G12V/K147L mutant of K-Ras co-localized with G12V-K-Ras at both the plasma membrane and intracellular membranes. However, a small population (< 5%) of cells had intracellular vesicles where only the G12V-K-Ras localized (fig, S3A). Since the K147L mutant is still ubiquitinated, these results do not address whether ubiquitination in general affects localization. However, they raise the possibility that ubiquitination at Lys^{147} occurs in a specific compartment or results in trafficking to a specific compartment where downstream signaling occurs.

To further investigate the impact of Ras ubiquitination on subcellular localization, we examined whether ubiquitinated forms of K-Ras differed from non-ubiquitinated forms in regard to their abilities to be extracted from cells by various concentrations of detergent and salt. The overall pattern of ubiquitinated G12V-K-Ras was very similar to non-ubiquitinated G12V-K-Ras, however fraction seven (1% NP40, 650mM NaCl extract) contained slightly less ubiquitinated K-Ras (fig, S3B). In contrast, ubiquitinated forms of H-Ras exhibited profound differences from non-ubiquitinated H-Ras in regard to extraction with detergent and salt (fig, S3B), which is consistent with previous reports (11, 12). Localization of H-Ras and N-Ras, but not K-Ras, is regulated by palmitoylation (1). Therefore, it is possible that a ubiquitinated-Ras binding protein could restrict access to the residue that is targeted for palmitoylation or inhibit the palmitoylation process, while K-Ras would be refractory to such regulation due to the lack of a palmitoylation site. These results suggest that ubiquitination of K-Ras does not globally affect its localization. However we could not rule out the possibility that these small fractions of ubiquitinated K-Ras play an important role in a site-specific manner.

K147L mutation in G12V-K-Ras reduces its tumorigenic activity

To examine the importance of Lys^{147} ubiquitination in Ras tumorigenic activity *in vivo*, we injected 3T3 cells expressing either G12V-K-Ras as a control or G12V/K147L double mutant K-Ras into the flank of immunocompromised nude mice. The expression levels of the control and the double mutant were comparable, and they did not exceed endogenous Ras levels (Fig. 5A). G12V/K147L-K-Ras cells were capable of forming tumors in nude mice. However, the volume and weight of G12V/K147L-K-Ras driven tumors was clearly less than that of the G12V-K-Ras driven tumors a week after injection (Fig. 5B and C). We further investigated the signaling status in these tumors. The phosphorylation of ERK and AKT were not substantially different in the two tumor types, though a small decrease in AKT phosphorylation was observed (Fig. 5D). However, due to negative feedback loops that suppress phosphorylation of these proteins, AKT phosphorylation level is not a very quantitative readout of flux through these pathways. We did observe that the G12V/K147L mutant tumors had a decrease in phospho-S6 (~18%), which is known to be downstream of both the PI3K and MAPK pathways and which typically correlates better with signaling downstream of Ras. It is possible, that the subset of cells in the G12V/K147L driven tumors that had very low PI3K and MAPK signaling failed to divide or died, hence explaining the reduced tumor size.

Although non-ubiquitinated G12V-KRas and G12V/K147L-KRas equally interacted with PI3K and Raf1, ubiquitinated G12V/K147L reduced its binding to PI3K but not Raf kinase (fig. S2B). This suggests the possibility that ubiquitination of a distinct lysine residue(s) enhances binding to specific effectors, and also that ubiquitination of K147 may not only increase the GTP-form but it also enhances the binding to PI3K, thus activating PI3K/AKT signaling, which contributes to the tumorigenic activity of Ras.

A kinetic Model predicts dynamic Ras ubiquitination

To study the consequences of Ras ubiquitination on directing specific downstream responses to Ras signaling, we calculated a phase map of the fraction of ubiquitinated Ras out of the total amount of Ras in its GTP-bound form as a function of the relative enzymatic activities of ubiquitination and de-ubiquitination. As shown in Fig. 6A, it is predicted that changes in ubiquitination activity affect signal discrimination nonlinearly such that small changes in ubiquitination activity can lead to large disproportional changes relative to the change in ubiquitination activity. This observation predicts that there are likely scenarios in different cellular contexts in which the relative amount of ubiquitination is more abundant. Furthermore, it is also predicted that small changes in deubiquitinating enzyme activity could lead to a disproportionate amount of enhanced effector signaling through the PI3K/AKT and Raf/ERK pathways. This model predicts cellular heterogeneity in signaling and is consistent with the observation that the G12V/K147L-K-Ras driven tumors are smaller and that the subset of cells that persist in these tumors have Ras pathway signaling that is not very different from that in the G12V-K-Ras driven tumors.

DISCUSSION

Ubiquitination is a dynamic, reversible modification conserved among all eukaryotic cells. Our present study has shed light on novel functions for ubiquitin, namely its capacity to increase the GTP-form of Ras as well as to increase the affinity of GTP-loaded Ras to certain effectors. We propose that once ubiquitination occurs on Ras at Lys^{147}, it enhances GDP/GTP exchange of Ras and increases the fraction of Ras in the GTP-form (Fig. 6B). The mechanism by which this occurs is not yet clear, but it is likely that ubiquitination at Lys^{147} enhances the release of GDP, since this residue directly binds to the guanine moiety of GDP and certain mutations at Lys^{147} also enhance K-Ras activation (Fig.1E). It is also possible that ubiquitination of Lys^{117} increases Ras GDP/GTP exchange, as Lys^{117} is also a critical residue for guanine recognition by Ras. In addition to its effect on GTP binding, ubiquitination of Ras also causes an enhanced interaction with the downstream effectors Raf, RalGDS and PI3K. Thus, although we were only able to precipitate a small amount of ubiquitinated G12V-K-Ras from cells, the amount of PI3K and Raf bound to this minor fraction was comparable to that bound to total G12V-K-Ras.

Ubiquitination of K-Ras is evolutionarily conserved, since Drosophila Ras, which is an orthologue of mammalian K-Ras, undergoes mono- and di-ubiquitination (30, 31). We found that endogenous K-Ras and H-Ras undergo mono- and di- ubiquitination in both HEK293T cells (Fig.1A) and U2OS cells (in preparation). However, ubiquitination of K-Ras was not detected in CHOK1 cells (11) raising the possibility that the E3 ligase that mediates K-Ras ubiquitination is not expressed in all tissues. Rabex5 specifically ubiquitinates H/N-Ras (12), but the E3 ligase(s) responsible for ubiquitinating K-Ras at Lys^{147} and Lys^{117} remain to be determined. It is possible that Rabex5-mediated Ras ubiquitination occurs at residues other than Lys^{147} and Lys^{117}, and this phenomenon abrogates Ras activity. Thus it is likely that differential expression or regulation of RasE3-ligases and deubiquitinating enzymes (DUBs) may control Ras ubiquitination to promote degradation, translocation or activation of specific Ras isoforms in specific tissues.

Our result (fig. S1) shows that T35A-mutant of K-Ras, which cannot bind to downstream effectors, still undergoes ubiquitination at a comparable level to wild type K-Ras. In addition, it has been shown that G12V-H-Ras and dominant negative S17N-H-Ras are ubiquitinated (11). These indicate that Ras ubiquitination occurs independently of its activity. However there are likely several Ras ubiquitination mechanisms as described above, which include the Ras activity dependent ubiquitination pathway (12).

Our results raise a number of important questions. What is the E3 ligase responsible for monoubiquitination at Lys^{147}, what is the deubiquitinating enzyme and are these enzymes regulated by any growth factor signaling pathways? Are mono-ubiquitination and activation of Ras ultimately linked to polyubiquitination and degradation of the same protein? We hypothesize that Ras stability varies in different cell types and cell contexts and this most likely depends on the balance between Ras-E2/E3-ligase and de-ubiquitinating enzyme activity (Fig. 6B). Finally, what fraction of total PI3K activation or total Raf activation in cells is a consequence of this mechanism? Is Ras ubiquitination involved in Ras addiction and in synthetic lethality? In any event, the small fraction of ubiquitinated K-Ras observed appears to account for a significant amount of the bound PI3K and Raf, raising the possibility that pharmaceutical disruption of this ubiquitination pathway could be beneficial in treating cancers with Ras mutations or other cancers where Ras activation is driving tumor growth and survival.

Materials and Methods

Materials

Flag-, Flag-His- (FH), GFP-, or RFP- tagged Ras mutants were generated by the standard polymerase chain reaction (PCR) method and subcloned into pCMV2, pEGFP-C3, or pRFP (monomer)-C3. Antibodies to EEA1 (H-300), GFP (FL), Raf1 (C-20), B-Raf (C-19), Tubulin (DM1A), Ubiquitin (P4D1) are from Santa Cruz; antibodies to Afadin (ab11338) GAPDH (ab9485), Lamin B (46048) and Calmodulin (EP799Y) are from Abcam; anti-Ras (Ab-3) is from EMD/Calbiochem; rabbit anti-K-Ras (12063) is from Protein Tech Group; anti-PI3K-p85 (N-SH2), anti-H-Ras (MAB3291) and anti-PLCε (07–513) are from Millipore/Upstate; anti-Calreticulin and rabbit anti-Ras (EP1125Y) are from Novus Biological; anti-TFP1 (3721) is from BioVision, Inc., anti-RalGDS antibody (1A11) is from Gene Tex, Inc., anti-Flag (M2) antibody and anti-Flag-agarose are from Sigma-Aldrich, biotinylated anti-HA (16B12) is from Couvance; Streptavidine-HRP conjugate is from GE Healthcare. Anti-mTOR (2972) and Biotinylated protein ladder are from Cell Signaling Technology. Bovine serum albumin (Fraction V) is from Sigma. Bis-Tris gels are from Invitrogen. Fugene 6 (Roche Applied Science) was used for all transfection. The anti-HA monoclonal antibody (16B12) was chosen as it recognizes poly-HA-ubiquitin faithfully (fig, S4). All western blot experiments have been done at least twice.

GST-RBD pull-down assay

Ras activation was measured as described previously (23). Briefly, cells were rinsed with cold PBS and lysed with Buffer A; 0.5 %NP-40, 40 mM HEPES [pH 7.4], 150 mM NaCl, 10 % glycerol, 1 mM DTT, 1 μg/ml leupeptin, 2 μg/ml aprotinin, 1 μg/ml pepstatin A, 100 μM AEBSF, and Halt phosphatase inhibitor cocktail (Thermo Scientific.) The soluble fraction of cell lysates were isolated by centrifugation at 14,000 rpm for 10 min and incubated with 10 μg of GSH-Sepharose bound GST-RBD in the presence of 1 mg/ml BSA for 30 min. For the ubiquitinated Ras assay, Flag-His-tagged K-Ras was co-expressed with HA-ubiquitin into HEK293T cells. The cells were lysed with Buffer A containing 10 mM iodoacetamide (IAA) and 5mM *N*-ethylmaleimide (NEM) and were split and subjected to anti-Flag agarose immunoprecipitation and the GST-RBD assay. The immunoprecipitated and pull-downed proteins were washed three times with Buffer A and eluted by the addition of 8M urea and further subjected to Co^{2+} Talon metal affinity chromatography (Clontech) to detect clear ubiquitinated Ras signal. The Flag-His-tagged Ras was eluted with sample buffer containing 50mM EDTA.

In vitro kinase assays

HA-ubiquitin and Flag-G12V-K-Ras transfected cells were rinsed with cold PBS and lysed with Buffer A containing 10 mM IAA and 5 mM NEM, and immunoprecipitated with agarose-conjugated anti-Flag (M2) antibody (Sigma). Immunoprecipitates were washed three times with Buffer A and once with Buffer B: 20 mM HEPES (pH7.4), 25 mM β-glycerol phosphate, 0.5 mM EGTA, 1mM sodium vanadate, and 1 mM dithiothreitol. The total Flag-K-Ras was obtained by elution with 100 μg/ml 3×Flag peptide in Buffer B (Sigma). To purify ubiquitinated K-Ras, the purified total K-Ras was incubated with anti-HA agarose (Sigma) for 1h and then washed three times with Buffer A and once with Buffer B. The Raf kinase assay was performed using GST-MEK and GST-ERK2 (Upstate biotechnology) as substrates in Buffer B containing 10 μCi of [γ-^{32}P] ATP, 100 μM cold ATP, and 25 mM magnesium chloride for 10 min at room temperature. Reaction products were resolved by SDS-PAGE, and phosphorylated GST-MEK1 and GST–ERK2 were analyzed by autoradiography. The PI3K assay was performed by adding 20 μl of HEPES (100 mM; pH 7), 20 μl of sonicated lipids (67 μM phosphoinositide) (PI; Avanti Polar Lipids), 133 μM phosphoserine (PS; Avanti Polar Lipids) and 10 μl of ATP mix (70 mM HEPES [pH 7], 50 mM $MgCl_2$, 0.5 mM ATP, [γ-^{32}P]ATP [10 μCi/assay mixture]) to 50 μl of immunoprecipitate. The reactions were performed at room temperature and stopped after 30 min by adding 25 μl of 5M HCl. The lipids were extracted with 160 μl of $CHCl_3$-MeOH (1:1). The phosphorylated lipids were spotted on a thin-layer chromatography (TLC) and separated overnight with 1-propanol-2M acetic acid (65:35). The radioactivity was visualized by autoradiography.

Measurement of GTP and GDP in Ras by TLC or HPLC

WT or G12V mutant Flag-Ras was co-transfected with HA-ubiquitin into HEK293T cells. The cells were labeled with [^{32}P]-inorganic phosphate, and total Flag-Ras and ubiquitinated Flag-Ras were purified as above. For TLC, the beads were incubated with elution buffer (0.2% SDS, 5mM DT, 1mM GDP, 1mM GTP, 2mM EDTA) and the eluted samples were spotted on PEI cellulose, 100 micron, 20 × 20 cm (Selecto Scientific, Inc.) and developed in 0.75M KH_2PO_4 (pH 3.4). The GTP and GDP level were quantified with a phosphoimager (Molecular Dynamics, STORM840). For HPLC analysis, the beads were incubated with PBS containing 50 mM $HClO_4$, and the nucleotide containing fraction was purified by mixed phase extraction employing 11.75:13.25 (vol/vol) of tri-n-octylamine (Sigma) and Freon 11 (Sigma). HPLC was performed using Agilent Technology 1200, a Zorbax Rx-C8 column (4 × 250 mm), buffer C; 50mM KH_2PO_4, 8mM tetrabutylammonium hydrogen sulfate (TBAS), and 40 % (vol/vol) acetonitrile at pH 5.8, Buffer D; 50 mM KH_2PO_4, 8 mM TBAS at pH 5.8. The radioactive samples were co-injected with standard cold 30 μM of GTP, GDP, and ATP (Sigma). ^{32}P-GTP and -GDP signals were detected by Packard Radiomatic Flo-one Beta Radioactive Flow Detector, and standard nucleotides were detected spectrophotometrically.

Tandem Mass Spectrometry Analysis

His-ubiquitin and Flag-K-Ras or Flag-H-Ras were transfected into HEK293T cells. Cells were rinsed with PBS and directly lysed with 8M urea and subjected to Co^{2+} Talon metal affinity purification (Clontech). The beads were washed with urea of 8, 6, 4, 2, 1, 0.5, 0.25, and 0.15 M sequentially. His-ubiquitinated proteins were purified with Buffer A containing 10 mM NEM and 50 mM EDTA, and ubiquitinated-Ras proteins were further purified with the anti-Flag agarose. Samples were prepared from SDS-PAGE gels, stained with Coomassie blue and excised for mass spectrometry sequencing and ubiquitin site mapping. Gel pieces were reduced with DTT, Cys residues were alkylated with iodoacetamide and digested overnight using modified trypsin (Promega) at 37°C at pH 8.3. Peptides were extracted and analyzed by data-dependent microcapillary tandem mass spectrometry (LC/

MS/MS) using both linear ion trap (Thermo Scientific, San Jose, CA) and a high resolution/mass accuracy hybrid linear ion trap LTQ-Orbitrap XL mass spectrometer (Thermo Scientific, San Jose, CA) coupled to an EASY-nLC nanoflow HPLC (Proxeon Biosystems). MS/MS spectra acquired via collision-induced dissociation (CID) were searched against the reversed and concatenated Swiss-Prot protein database (v. 55.8, UniProt) with a fixed modification for carbamidomethylation (+57.0293) and the variable modifications for oxidation (+15.9949) and ubiquitination (+114.10, GG tag) using the Sequest algorithm in Proteomics Browser Software (Thermo Scientific). Peptides from K-Ras and H-Ras and were identified by database scoring and peptides modified by ubiquitin were validated manually to be sure that all **b**- and **y**- series ions were consistent with the modified residue and additional validation was performed using GraphMod software in Proteomics Browser Software (Thermo Scientific). The peptide false discovery rate (FDR) was less than 1.5% based on reversed database hits.

Xenograft assay

7 million NIH-3T3 cells expressing either G12V-K-Ras or G12V/K147L-K-Ras were injected with matrigel HC (BD Pharmingen) into the flank of Nude mice. Tumors were measured at days 5, 6 and 7 after injection. At day 7, mice were euthanized and tumors were harvested, weighed, and processed for analysis.

Confocal microscope analysis

Confocal images were obtained by using CSU10 spinning disk confocal (Yokogawa) on a Nikon Ti inverted microscope with a 63×/1.4 objective using an ORCA-AG cooled CCD camera (Hamamatsu). The images were acquired and analyzed by MetaMorph.

Statistics

Statistical analysis was performed by ANOVA with a post-hoc analysis using the Student-Neuman-Keuls test. Differences were considered significant when the P value was less than 0.05.

Structural analysis

Structural alignments and visualization of H-Ras (2CE2) and Rac1 (1MH1) were created using the program PyMOL (http://pymol.org/).

Supplementary Material

Refer to Web version on PubMed Central for supplementary material.

Acknowledgments

We gratefully acknowledge the members of the Cantley laboratory and the Izayoi Meeting for stimulating discussions and helpful suggestions, Drs. Yu-Hsin Chiu, Yoko Saikawa, Fumihiko Okumura and Satoshi Yoshida for critical comments, Xuemei Yang for help with mass spectrometry experiments for excellent technical assistance and Edouard Mullarky, Mika Sasaki for help in preparing this manuscript. We thank the Nikon Imaging Center at Harvard Medical School for help with imaging. ATS was supported, in part, by the Japanese Society for the Promotion of Science Research Fellowship for Research Abroad, Kanae foundation for Research Abroad, and a Genentech Fellowship. AC was supported by the EMBO long-term fellowship and the Ramón y Cajal Prize, JWL was supported by a fellowship from the American Cancer Society. This work was funded by research grants R01-GM41890, 5P01CA117969 and P01CA089021 to LCC and NIH grants 1P01CA120964-01A1 and 5P30CA006516-43 to JMA.

REFERENCES

1. Karnoub AE, Weinberg RA. Ras oncogenes: split personalities. Nat Rev Mol Cell Biol. 2008; 9:517–531. [PubMed: 18568040]
2. Wennerberg K, Rossman KL, Der CJ. The Ras superfamily at a glance. J Cell Sci. 2005; 118:843–846. [PubMed: 15731001]
3. Vetter IR, Wittinghofer A. The guanine nucleotide-binding switch in three dimensions. Science. 2001; 294:1299–1304. [PubMed: 11701921]
4. Edkins S, O'Meara S, Parker A, Stevens C, Reis M, Jones S, Greenman C, Davies H, Dalgliesh G, Forbes S, Hunter C, Smith R, Stephens P, Goldstraw P, Nicholson A, Chan TL, Velculescu VE, Yuen ST, Leung SY, Stratton MR, Futreal PA. Recurrent KRAS codon 146 mutations in human colorectal cancer. Cancer Biol Ther. 2006; 5:928–932. [PubMed: 16969076]
5. Schubbert S, Bollag G, Lyubynska N, Nguyen H, Kratz CP, Zenker M, Niemeyer CM, Molven A, Shannon K. Biochemical and functional characterization of germ line KRAS mutations. Mol Cell Biol. 2007; 27:7765–7770. [PubMed: 17875937]
6. Denayer E, Parret A, Chmara M, Schubbert S, Vogels A, Devriendt K, Frijns JP, Rybin V, de Ravel TJ, Shannon K, Cools J, Scheffzek K, Legius E. Mutation analysis in Costello syndrome: functional and structural characterization of the HRAS p.Lys117Arg mutation. Hum Mutat. 2008; 29:232–239. [PubMed: 17979197]
7. Janakiraman M, Vakiani E, Zeng Z, Pratilas CA, Taylor BS, Chitale D, Halilovic E, Wilson M, Huberman K, Ricarte Filho JC, Persaud Y, Levine DA, Fagin JA, Jhanwar SC, Mariadason JM, Lash A, Ladanyi M, Saltz LB, Heguy A, Paty PB, Solit DB. Genomic and biological characterization of exon 4 KRAS mutations in human cancer. Cancer Res. 2010; 70:5901–5911. [PubMed: 20570890]
8. Morrison DK, Davis RJ. Regulation of MAP kinase signaling modules by scaffold proteins in mammals. Annu Rev Cell Dev Biol. 2003; 19:91–118. [PubMed: 14570565]
9. Elion EA. The Ste5p scaffold. J Cell Sci. 2001; 114:3967–3978. [PubMed: 11739629]
10. Li W, Han M, Guan KL. The leucine-rich repeat protein SUR-8 enhances MAP kinase activation and forms a complex with Ras and Raf. Genes Dev. 2000; 14:895–900. [PubMed: 10783161]
11. Jura N, Scotto-Lavino E, Sobczyk A, Bar-Sagi D. Differential modification of Ras proteins by ubiquitination. Mol Cell. 2006; 21:679–687. [PubMed: 16507365]
12. Xu L, Lubkov V, Taylor LJ, Bar-Sagi D. Feedback regulation of Ras signaling by Rabex-5-mediated ubiquitination. Curr Biol. 2010; 20:1372–1377. [PubMed: 20655225]
13. Kim SE, Yoon JY, Jeong WJ, Jeon SH, Park Y, Yoon JB, Park YN, Kim H, Choi KY. H-Ras is degraded by Wnt/beta-catenin signaling via beta-TrCP-mediated polyubiquitylation. J Cell Sci. 2009; 122:842–848. [PubMed: 19240121]
14. Spoerner M, Herrmann C, Vetter IR, Kalbitzer HR, Wittinghofer A. Dynamic properties of the Ras switch I region and its importance for binding to effectors. Proc Natl Acad Sci U S A. 2001; 98:4944–4949. [PubMed: 11320243]
15. Thrower JS, Hoffman L, Rechsteiner M, Pickart CM. Recognition of the polyubiquitin proteolytic signal. Embo J. 2000; 19:94–102. [PubMed: 10619848]
16. Miller J, Gordon C. The regulation of proteasome degradation by multi-ubiquitin chain binding proteins. FEBS Lett. 2005; 579:3224–3230. [PubMed: 15943965]
17. Sjoblom T, Jones S, Wood LD, Parsons DW, Lin J, Barber TD, Mandelker D, Leary RJ, Ptak J, Silliman N, Szabo S, Buckhaults P, Farrell C, Meeh P, Markowitz SD, Willis J, Dawson D, Willson JK, Gazdar AF, Hartigan J, Wu L, Liu C, Parmigiani G, Park BH, Bachman KE, Papadopoulos N, Vogelstein B, Kinzler KW, Velculescu VE. The consensus coding sequences of human breast and colorectal cancers. Science. 2006; 314:268–274. [PubMed: 16959974]
18. Sloan SR, Newcomb EW, Pellicer A. Neutron radiation can activate K-ras via a point mutation in codon 146 and induces a different spectrum of ras mutations than does gamma radiation. Mol Cell Biol. 1990; 10:405–408. [PubMed: 2403644]
19. Orita S, Higashi T, Kawasaki Y, Harada A, Igarashi H, Monden T, Morimoto H, Shimano T, Mori T, Miyoshi J. A novel point mutation at codon 146 of the K-ras gene in a human colorectal cancer identified by the polymerase chain reaction. Virus Genes. 1991; 5:75–79. [PubMed: 2017878]

20. Zampino G, Pantaleoni F, Carta C, Cobellis G, Vasta I, Neri C, Pogna EA, De Feo E, Delogu A, Sarkozy A, Atzeri F, Selicorni A, Rauen KA, Cytrynbaum CS, Weksberg R, Dallapiccola B, Ballabio A, Gelb BD, Neri G, Tartaglia M. Diversity, parental germline origin, and phenotypic spectrum of de novo HRAS missense changes in Costello syndrome. Hum Mutat. 2007; 28:265–272. [PubMed: 17054105]
21. Milburn MV, Tong L, deVos AM, Brunger A, Yamaizumi Z, Nishimura S, Kim SH. Molecular switch for signal transduction: structural differences between active and inactive forms of protooncogenic ras proteins. Science. 1990; 247:939–945. [PubMed: 2406906]
22. Pai EF, Krengel U, Petsko GA, Goody RS, Kabsch W, Wittinghofer A. Refined crystal structure of the triphosphate conformation of H-ras p21 at 1.35 A resolution: implications for the mechanism of GTP hydrolysis. Embo J. 1990; 9:2351–2359. [PubMed: 2196171]
23. Sasaki AT, Firtel RA. Spatiotemporal regulation of Ras-GTPases during chemotaxis. Methods Mol Biol. 2009; 571:333–348. [PubMed: 19763978]
24. Lopez-Alcala C, Alvarez-Moya B, Villalonga P, Calvo M, Bachs O, Agell N. Identification of essential interacting elements in K-Ras/calmodulin binding and its role in K-Ras localization. J Biol Chem. 2008; 283:10621–10631. [PubMed: 18182391]
25. Chen Z, Otto JC, Bergo MO, Young SG, Casey PJ. The C-terminal polylysine region and methylation of K-Ras are critical for the interaction between K-Ras and microtubules. J Biol Chem. 2000; 275:41251–41257. [PubMed: 11007785]
26. Boettner B, Govek EE, Cross J, Van Aelst L. The junctional multidomain protein AF-6 is a binding partner of the Rap1A GTPase and associates with the actin cytoskeletal regulator profilin. Proc Natl Acad Sci U S A. 2000; 97:9064–9069. [PubMed: 10922060]
27. Hu CD, Kariya K, Tamada M, Akasaka K, Shirouzu M, Yokoyama S, Kataoka T. Cysteine-rich region of Raf-1 interacts with activator domain of post-translationally modified Ha-Ras. J Biol Chem. 1995; 270:30274–30277. [PubMed: 8530446]
28. Drugan JK, Khosravi-Far R, White MA, Der CJ, Sung YJ, Hwang YW, Campbell SL. Ras interaction with two distinct binding domains in Raf-1 may be required for Ras transformation. J Biol Chem. 1996; 271:233–237. [PubMed: 8550565]
29. Brtva TR, Drugan JK, Ghosh S, Terrell RS, Campbell-Burk S, Bell RM, Der CJ. Two distinct Raf domains mediate interaction with Ras. J Biol Chem. 1995; 270:9809–9812. [PubMed: 7730360]
30. Yan H, Chin ML, Horvath EA, Kane EA, Pfleger CM. Impairment of ubiquitylation by mutation in Drosophila E1 promotes both cell-autonomous and non-cell-autonomous Ras-ERK activation in vivo. J Cell Sci. 2009; 122:1461–1470. [PubMed: 19366732]
31. Yan H, Jahanshahi M, Horvath EA, Liu HY, Pfleger CM. Rabex-5 ubiquitin ligase activity restricts Ras signaling to establish pathway homeostasis in Drosophila. Curr Biol. 20:1378–1382. [PubMed: 20655224]

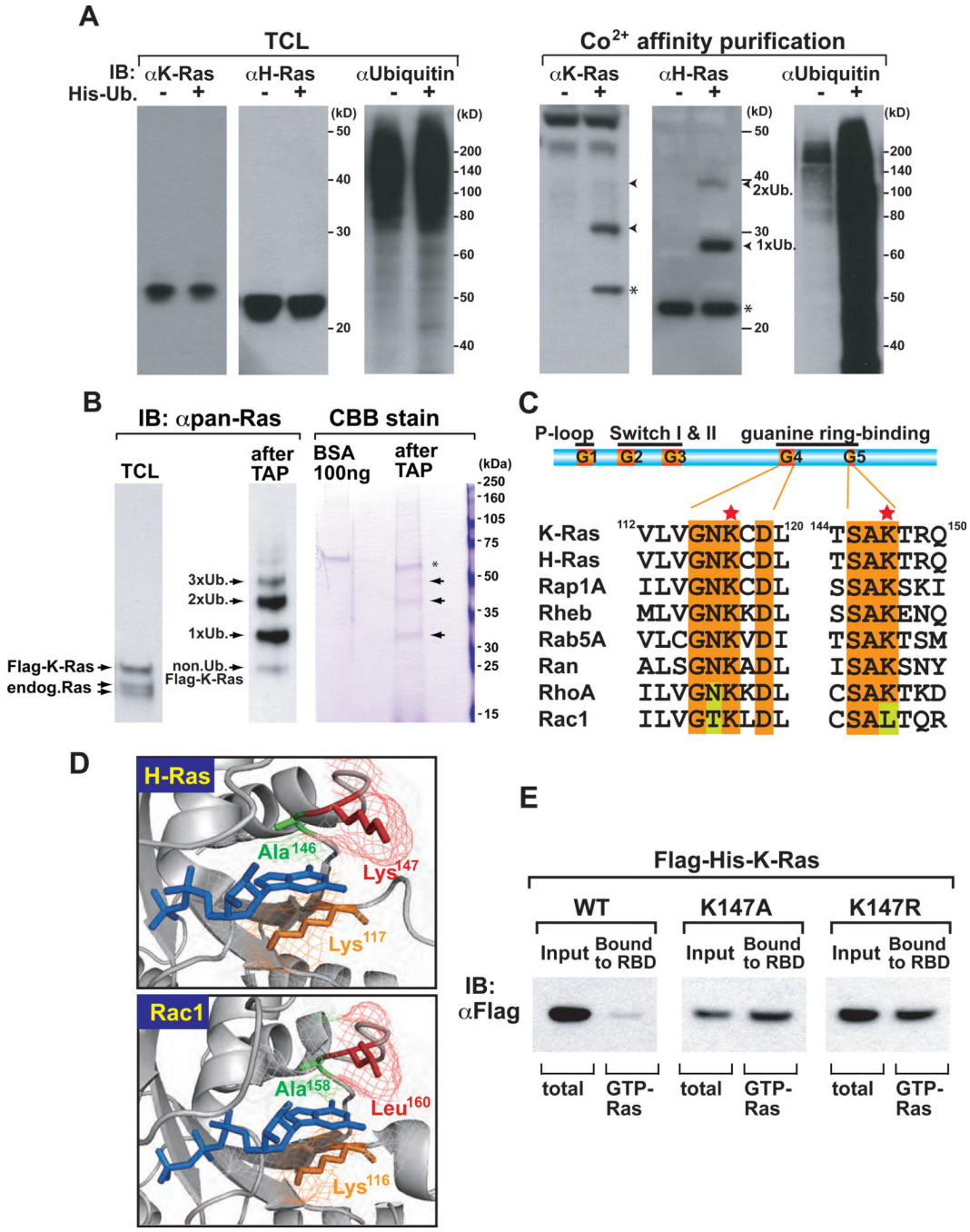

Figure 1. Lysine-147 is one of the major ubiquitination sites of K-Ras and H-Ras

(A) Endogenous K-Ras and H-Ras undergo mono- and di- ubiquitination in HEK293T cells. His-ubiquitinated proteins were enriched from total cell lysates (TCL) of His-tagged ubiquitin expressing cells or non-expressing cells by Co^{2+} affinity purification, and immunoblotted (IB) with the indicated antibodies. K-Ras migrates slower than H-Ras in SDS-PAGE. Ubiquitinated Ras is indicated with arrowheads. The asterisk indicates non-ubiquitinated Ras, which could be contamination or a de-ubiquitinated product formed after the purification by deubiquitinating enzymes. (B) Coomassie Brilliant Blue (CBB)-stainable ubiquitinated Ras was purified by tandem affinity purification for mass spectrometry analysis. His-ubiquitin and Flag-K-Ras were co-transfected in HEK293T cells and

ubiquitinated K-Ras was purified by tandem affinity purification (TAP) with a Co^{2+} column and anti-Flag resin. Isolated K-Ras was visualized with anti-Ras antibody or by CBB staining. The asterisk indicates a non-specific protein. (C) Schematic diagram of G-domain of Ras (upper). The identified ubiquitination sites, Lys^{117} and Lys^{147} are located in the G4 and G5 boxes and the corresponding regions in other representative small GTPases are aligned (lower). (D) Ras Lys^{117} (orange), A146 (green) and Lys^{147} (red), interact with the guanine moiety of the nucleotide. Rac1 uses leucine instead of lysine in its G5 box for guanine binding. (E) Disruption of the G5-box by mutating Lys^{147} to alanine or arginine increases the GTP-form of Ras. K-Ras wild-type (WT) or mutants were expressed in HEK293T cells, and their activation level was analyzed by a GST-RBD pull-down assay of Ras (see Materials and Methods). These blots are representative of three separate experiments

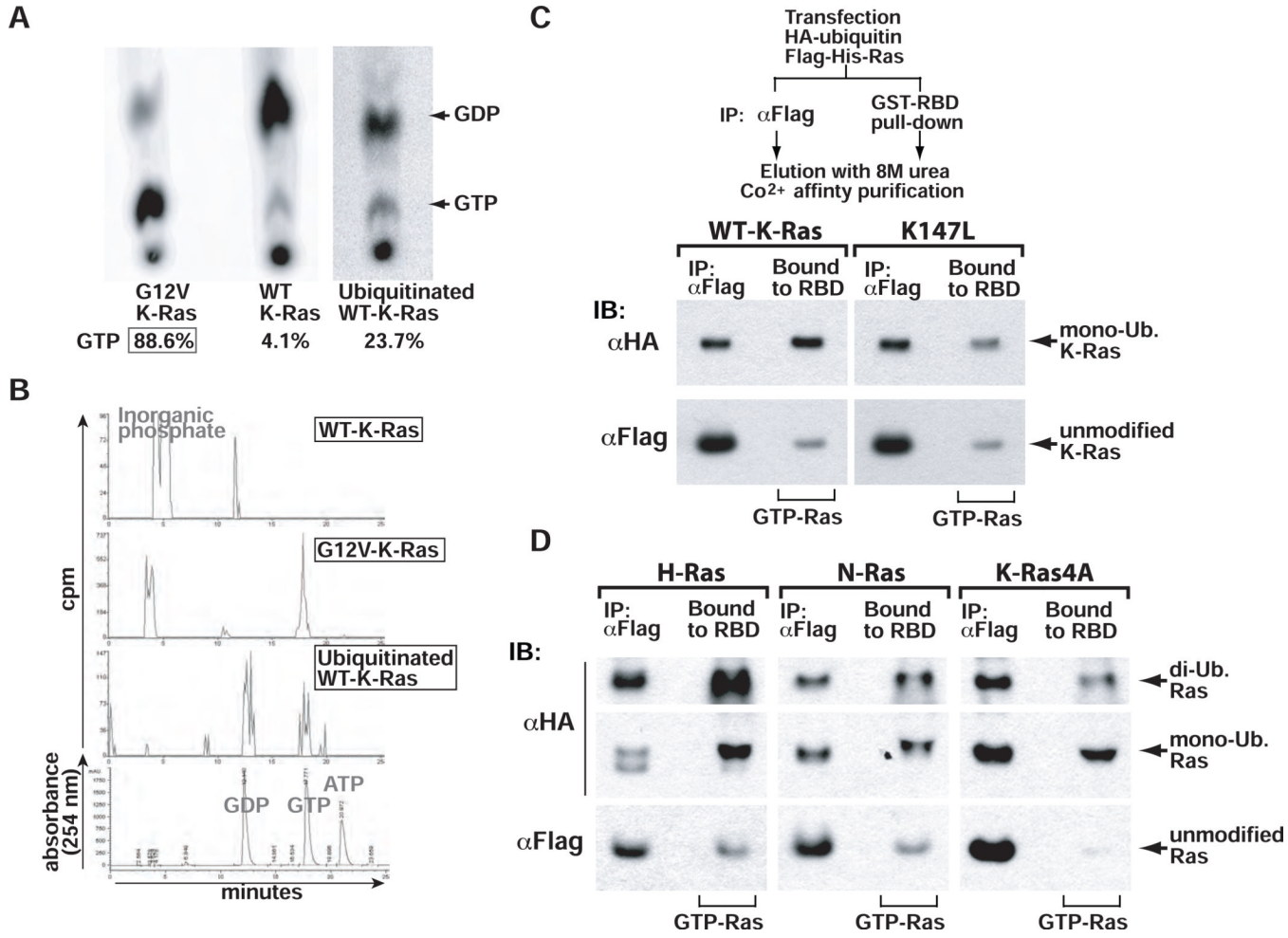

Figure 2. Ubiquitination of K147, a conserved lysine in the G5 box, increases the fraction of GTP-bound Ras

(A and B) Ubiquitination of K-Ras increases its GTP-form. WT-K-Ras, G12V-K-Ras, and ubiquitinated WT-K-Ras were purified from ^{32}P-phosphate labeled cells and the relative quantities of ^{32}P-GTP and ^{32}P-GDP co-purifying with each Ras species was determined by TLC (A) and HPLC (B). (C) Ubiquitination at Lys^{147} increased the binding of WT K-Ras to the RBD. Either Flag-His-tagged WT-K-Ras or K147L-K-Ras mutant were co-expressed with HA-tagged ubiquitin in HEK293 cells. The Ras proteins were either immunoprecipitated with an anti-Flag antibody or were pulled down with GST- RBD. Each precipitate was then dissolved in 8 M urea and further purified on a Co^{2+} affinity column to eliminate the antibody and GST-RBD contamination. Western blots with anti-Flag and anti-HA antibodies revealed the relative fraction of total K-Ras and that of the mono-ubiquitinated K-Ras species. GST-RBD was more efficient than anti-Flag antibody in precipitating the mono-ubiquitinated WT-K-Ras but was less efficient in precipitating the mono-ubiquitinated K147L mutant of K-Ras (upper panels). In contrast, GST-RBD was far less efficient than anti-Flag antibody in precipitating the non-ubiquitinated forms of both WT-K-Ras and K147L-K-Ras. These results are representative of two separate experiments. (D) Mono- and di- ubiquitinated Ras isoforms increased in their GTP-forms. Flag-His-tagged wild-type H-Ras, N-Ras, and K-Ras4A were expressed with HA-ubiquitin and analyzed as described in C. These results are representative of two separate experiments.

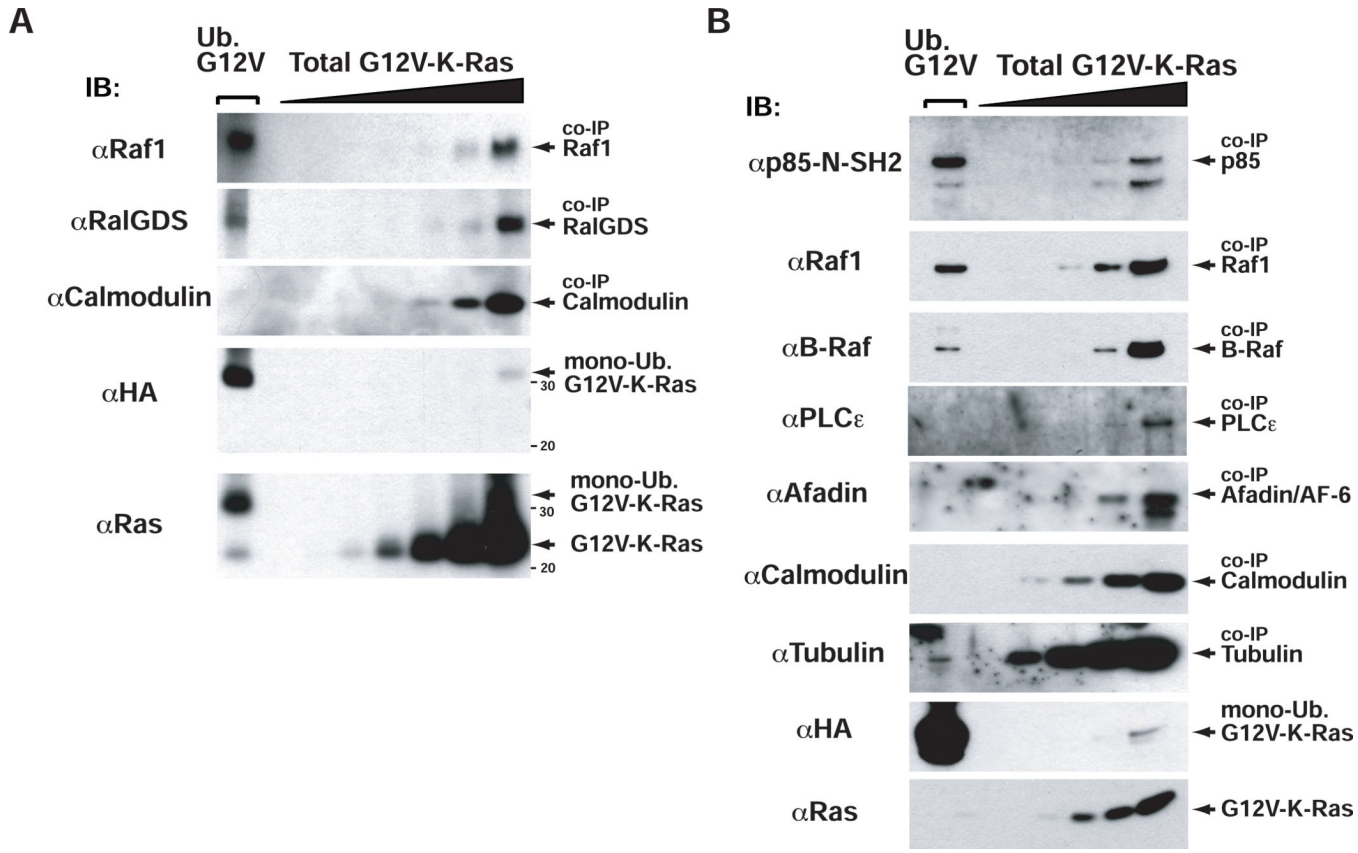

Figure 3. Raf and PI3K bind more to ubiquitinated Ras than to non-ubiquitinated Ras

Ubiquitinated G12V-K-Ras shows enhanced binding specifically to Rafs and PI3K. (A and B) Flag-K-Ras and HA-ubiquitin were co-expressed in HEK293T cells. The total K-Ras complex was immunoprecipitated with anti-Flag resin and eluted with Flag peptides. Ubiquitinated K-Ras was further purified with anti-HA agarose. Assays were performed on a series of dilutions of the eluate from the anti-Flag I.P. in order to compare the ratio of associated Ras effectors to the total K-Ras in comparable amounts of the ubiquitinated and non-ubiquitinated forms. Endogenous K-Ras binding proteins were detected with the indicated antibodies. These results are representative of two separate experiments.

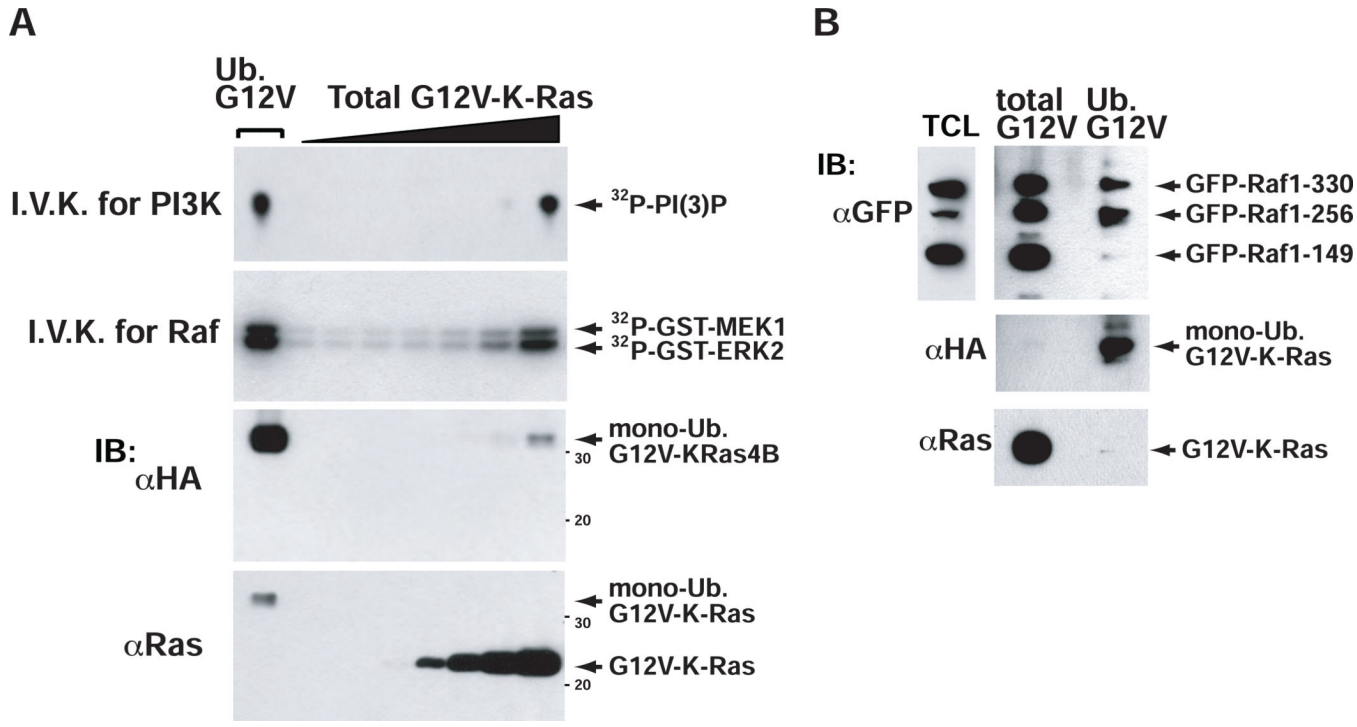

Figure 4. Ubiquitinated Ras activates Raf and PI3K more than non-ubiquitinated Ras

(A) The Ras-associated kinase activities of Raf and PI3K were compared by *in vitro* kinase assays (I.V.K; see Experimental Procedures). Aliquots of total Flag-G12V-K-Ras and ubiquitinated K-Ras prepared in Fig. 3A were used. The ratios of PI 3-kinase and Raf kinase activities to K-Ras protein were much higher for the mono-ubiquitinated protein, consistent with the enhanced binding of Raf and PI3K. (B) A C-terminal extended region of RBD confers enhanced binding to ubiquitinated K-Ras. Three different GFP-tagged Raf deletion mutants (1–149, 1–256 and 1–330) were simultaneously co-transfected with Flag-K-Ras and HA-ubiquitin in HEK293T cells. The total Flag-G12V-K-Ras and ubiquitinated K-Ras were precipitated as described in Fig. 3 and the relative quantity of the three deletion mutants was determined by western blotting with anti-GFP antibody. Total G12V-K-Ras bound all three Raf deletion mutants similarly while the ubiquitinated Raf preferentially bound to the two larger deletion mutants. A blot is representative of two separate experiments.

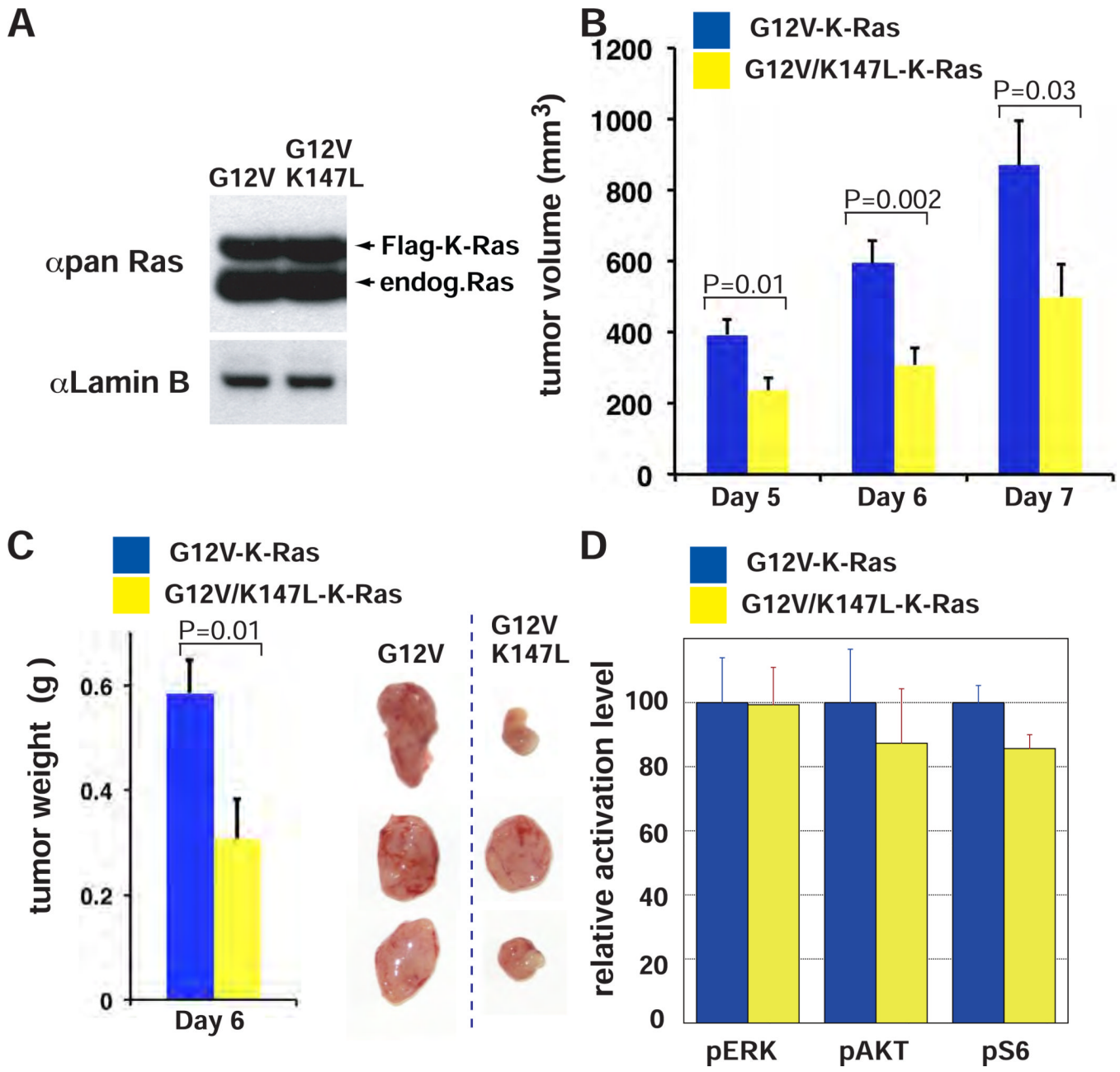

Figure 5. Modification of Lys^{147} is important for tumorigenic activity of G12V-K-Ras

(A) Flag-His tagged G12V-K-Ras or G12V/K147L-K-Ras were stably expressed in NIH3T3 cells and injected into each flank of eight nude mice. The total cell lysates of these NIH3T3 cells were immunoblotted with the indicated antibodies. Tumor volume (B) and weight (C) of G12V/K147L-K-Ras were significantly smaller than that of G12V-K-Ras tumors. Tumors dissected from the nude mice are shown (C-right). (D) G12V/K147L-K-Ras-induced tumors reduce PI3K/AKT signaling but retain Raf/ERK signaling. The tumors derived from G12V/K147L-K-Ras or G12V-K-Ras nude mice (at day seven) were lysed in RIPA buffer and extracted proteins were analyzed by LICOR infrared imaging which allows quantification of the relevant Western signals. The phospho-ERK, AKT (S473) and S6 levels from eight

tumors were normalized against total ERK, AKT, and S6, and plotted as relative activation level.

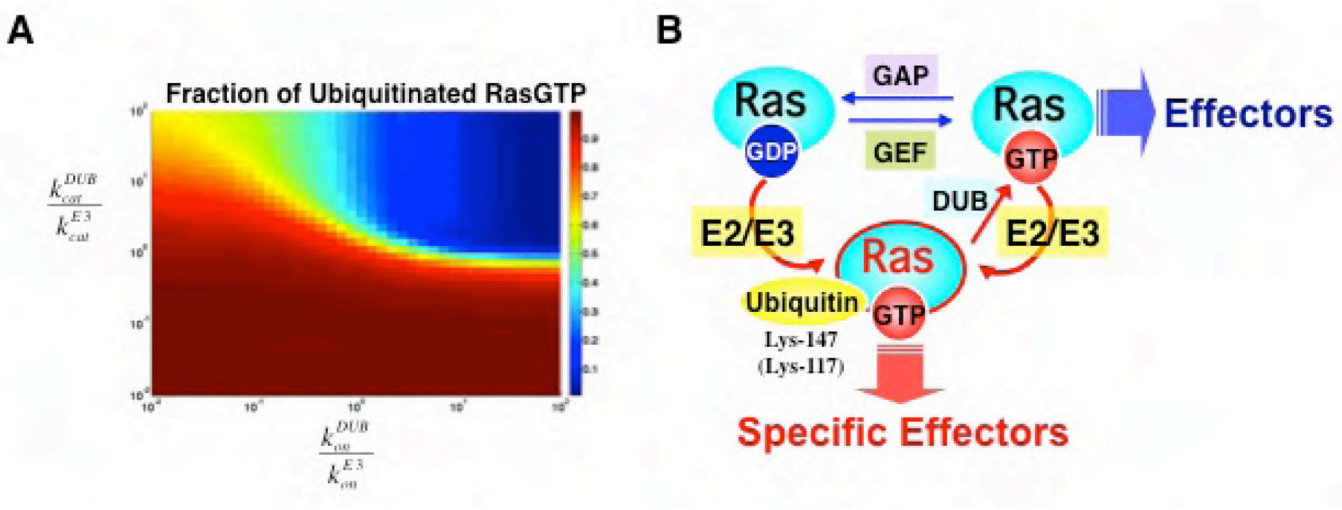

Figure 6. Model for ubiquitin-mediated Ras regulation

(A) Kinetic Model of Ras ubiquitination. The computational analysis suggests that, while small in our observations, the fraction of ubiquitinated Ras that affects cellular processes can be regulated by small changes in the rates ubiquitination and deubiquitination (detailed in the Supplemental information section). (B) Model for ubiquitin-mediated Ras regulation. The level of GTP and GDP Ras is regulated by GEFs and GAPs. In addition, our results suggest that ubiquitination of GDP-Ras at Lys^{117} or Lys^{147} induces GTP-loading. Also ubiquitination can directly occur on GTP-Ras. Ubiquitinated GTP-Ras interacts with specific effectors, such as Raf, PI3K and RalGDS, to modulate signaling. Ubiquitinated GTP-Ras could be reverted to non-ubiquitinated GTP-Ras by deubiquitinating enzymes (DUBs).